AN ANALYTICAL APPROACH TO HEAT TRANSFER FOR SLUG FLOW IN PARALLEL PLATES SUBJECTED TO CONSTANT WALL TEMPERATURE

MUHAMMAD ABDULLAH ZAFAR GHAURI[1] *

Abstract. This document presents an analytical investigation of heat transfer characteristics in a laminar slug flow about both sides of a parallel subjected to constant wall temperature. The study emphasizes on the undeveloped hydrodynamic boundary layer about the entrance region of pipe, where the velocity is approximated to be uniform. For low-Prandtl number fluids, $Pr < 1$, thermal diffusivity dominates over momentum diffusivity, thus justifying the neglect of axial conduction and viscous dissipation, The energy equation is solved using variable separation method, resulting in dimensionless temperature distribution.

Keywords. hydrodynamic boundary layer, Prandtl number, thermal diffusivity

1. Parallel: Slug Flow Heat Transfer in the Entrance Region

Slug flow is defined as fluid flow in the pipe regime where small air bubble transform to large air bubbles, filling the entire pipe cross-section, with liquid slugs containing smaller entrained gas bubbles present between them. Slug flows are typically observed at low values of Prandtl number.

Considering the short unheated entrance length of tube, with small value of Prandtl number (Pr$<$ 1), where $\delta/\Delta \to 1$, implies that the momentum boundary layer can be ignored from analysis in comparison with the thermal boundary layer. The rate of development of temperature profile is faster than that of velocity profile. With this, the axial velocity can be assumed to be constant and it can be approximated as

$$v_z = V$$

where V is the average fluid velocity. The said assumption is valid only for small value of entrance length and it is not valid for large distances downstream since the velocity profile shall ultimately develop.

One may consider the two-dimensional,incompressible, steady laminar flow of a low-Prandtl number fluid flowing in the entrance region of two parallel plates as seen in 1 The fluid properties are assumed to be constant, with negligible viscous dissipation and no internal energy generation. The pipe radius is denoted as R, where the fluid enters the pipe with an initial temperature of T_i and uniform velocity V. The flow is for low-Prandtl number, where $\delta/\Delta \to 1$, the rate of

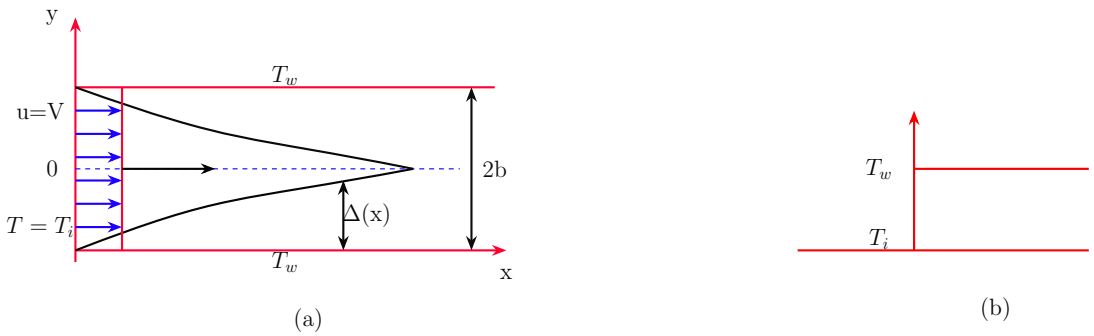


FIGURE 1. Slug flow between parallel plates (a) Thermal boundary layer development (b) Temperature distribution

development of temperature profile is faster than that of velocity profile, implying greater effect of diffusivity. With this, the axial velocity can be assumed to be constant and it can be approximated as $v_z = V$. The coordinate system is located at the duct inlet where the heating begins progressively. Heat flow gradually transforms into slug flow from the thermal pipe wall, which is maintained at constant temperature T_w. The area of duct is constant and thus, is heated about the entire length. The thermal boundary layer propagates from the entrance of duct and gradually develops along the entire length. Axial conduction and viscous dissipation are ignored from the analysis, with no energy generation. The temperature distribution and the empirical relation for the Nusselt number is to be determined.

In view of the assumptions made above, the energy equation at the entrance region is to be calculated as

$$\rho c_p V \frac{\partial T}{\partial x} = k \frac{\partial^2 T}{\partial y^2} \tag{1.1}$$

The corresponding boundary conditions are

$$T(0, y) = T_i \tag{1.2}$$

$$T(x, b) = T_w \tag{1.3}$$

$$\frac{\partial T(x, 0)}{\partial y} = 0 \tag{1.4}$$

The dimensionless variables for broader analysis can be defined here as

$$\theta = \frac{T(x, y) - T_w}{T_i - T_w} \tag{1.5}$$

$$\eta = \frac{y}{b} \tag{1.6}$$

$$x^+ = \frac{4(x/b)}{Re_{D_H} Pr} = \frac{4(x/b)}{Pe} \tag{1.7}$$

where $Re_{D_H} = \frac{\rho D_H V}{\mu}$ is the Reynolds number, $Pr = \frac{\mu c_p}{k}$ is the Prandtl number, $D_H = 4b$ is the hydraulic diameter and $Pe = Re_{D_H} Pr$ is the Peclet number. For

values of Peclet number less than 100, $Pe < 100$, axial conduction can be ignored [2]. The energy equation (Eq. 1.1) can be expressed as

$$\frac{\partial \theta}{\partial x^+} = \frac{\partial^2 \theta}{\partial \eta^2} \tag{1.8}$$

and the boundary conditions take the following shape

$$\begin{aligned} x^+ = 0 \qquad & \theta = 1 \\ x^+ > 0 \qquad & \eta = 0 \qquad \frac{\partial \theta}{\partial \eta} = 0 \quad \text{(Symmetry)} \\ x^+ > 0 \qquad & \eta = 1 \qquad \theta = 0 \end{aligned}$$

The solution of Eq. 1.7 can be obtained through separation of variables. Considering product solution in the following form:

$$\theta = X(x^+)Y(\eta)$$

Substitution of above in Eq. 1.7 after dividing both sides by $X(x^+)Y(\eta)$ results in

$$\frac{1}{X}\frac{dX}{dx^+} = \frac{1}{Y}\frac{d^2Y}{d\eta^2} = -\lambda^2 \tag{1.9}$$

From Eq.1.9

$$\frac{d^2Y}{d\eta^2} + \lambda^2 Y = 0 \tag{1.10}$$

The boundary conditions associated with above equation are

$$Y^{'}(0) = 0$$
$$Y(1) = 0$$

The eigenvalues and nontrivial eigenfunctions are

$$Y_n = B_n cos(\lambda_n \eta) \tag{1.11}$$

$$cos(\lambda_n) = 0 \qquad \lambda_n = (2n+1)\frac{\pi}{2} \qquad \forall n = 0, 1, 2, 3 \ldots$$

The differential equation in x^+-direction is

$$\frac{1}{X}\frac{dX}{dx^+} = -\lambda^2 \tag{1.12}$$

The solution for the above is

$$X_n = A_n \exp(-\lambda_n^2 x^+) \tag{1.13}$$

Thus, the product solution is

$$\theta(\xi, \eta) = \sum_{n=0}^{\infty} a_n \exp(-\lambda_n^2 x^+) cos(\lambda_n \eta) \tag{1.14}$$

where $a_n = A_n B_n$. Using the nonhomogenous boundary condition for evaluating the unknown constant a_n

$$1 = \sum_{n=0}^{\infty} a_n cos(\lambda_n \eta) \tag{1.15}$$

Eq. 1.15 is a Fourier cosine expansion of 1 across an interval (0,1). The unknown coefficient a_n is evaluated as

$$a_n = \frac{\int_0^1 cos(\lambda_n \eta) d\eta}{\int_0^1 cos^2(\lambda_n \eta) d\eta} = (-1)^n \frac{2}{\lambda_n} \tag{1.16}$$

By incorporating Eq. 1.16 in Eq. 1.14, the temperature distribution equation becomes

$$\theta(\xi, \eta) = 2 \sum_{n=0}^{\infty} \frac{(-1)^n}{\lambda_n} \exp(-\lambda_n^2 x^+) cos(\lambda_n \eta) \tag{1.17}$$

The mean fluid temperature is given as

$$T_m = \frac{\int_0^b uTdy}{\int_0^b udy} = \frac{1}{b} \int_0^b Tdy \tag{1.18}$$

Substituting $T = T_w + (T_i - T_w)\theta$ in Eq. 1.18, the mean fluid temperature can be evalauted as

$$T_m = \frac{1}{b} \int_o^b [T_w + (T_i - T_w)\theta] dy \tag{1.19}$$

In dimensionless variable form

$$\theta_m = \frac{T_m - T_w}{T_i - T_w} = \int_0^1 \theta d\eta \tag{1.20}$$

Substitution of dimensionless temperature distribution θ in Eq. 1.20 results in

$$\theta_m = \frac{T_m - T_w}{T_i - T_w} = 2 \sum_{n=0}^{\infty} \frac{\exp(-\lambda_n^2 x^+)}{\lambda_n^2} \tag{1.21}$$

Using the temperature distribution and mean fluid temperature, the Nusselt number can be determined using the hydraulic diameter $D_H = 4b$ as

$$h = \frac{q_w^{"}}{(T_w - T_m)} = -\frac{k \left(\frac{\partial T}{\partial y}\right)_{y=b}}{(T_w - T_m)} = -\frac{k \frac{(T_i - T_w)}{b} \left[\left(\frac{\partial \theta}{\partial \eta}\right)\right]_{\eta=1}}{(T_w - T_m)} \tag{1.22}$$

$$[\left(\frac{\partial \theta}{\partial \eta}\right)_{\eta=1} = 2 \sum_{n=0}^{\infty} \frac{(-1)^n}{\lambda_n} \exp(-\lambda_n^2 x^+) [-\lambda_n sin(\lambda_n \eta)]_{\eta=1}$$

$$\left(\frac{\partial \theta}{\partial \eta}\right)_{\eta=1} = 2 \sum_{n=0}^{\infty} \exp(-\lambda_n^2 x^+) \tag{1.23}$$

The local Nusselt number can be expressed as

$$Nu_{D_H} = \frac{hD_H}{k} = \frac{4 \sum_{n=0}^{\infty} \exp(-\lambda_n^2 x^+)}{\sum_{n=0}^{\infty} \frac{\exp(-\lambda_n^2 x^+)}{\lambda_n^2}} \tag{1.24}$$

The above analytical solution is interpreted in MATLAB 2025 for evaluating various plots including dimensionless temperature distribution, local Nusselt's number distribution etc.

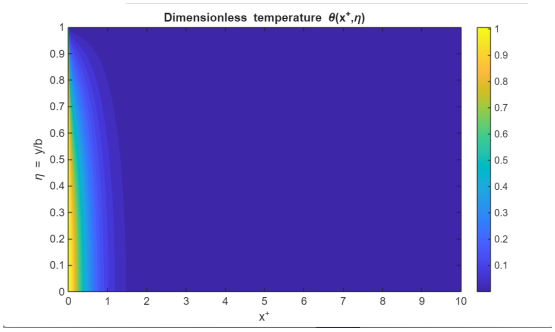


FIGURE 2. Contour for dimensionless temperature $\theta(x^+, \eta)$

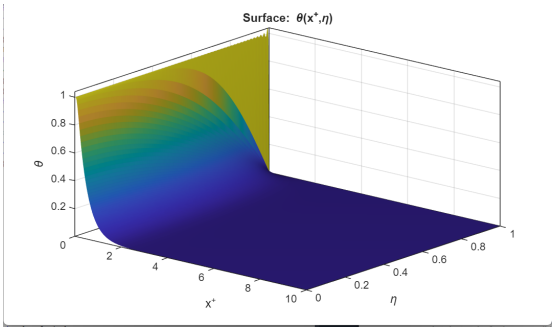


FIGURE 3. Surface contour for dimensionless temperature $\theta(x^+, \eta)$

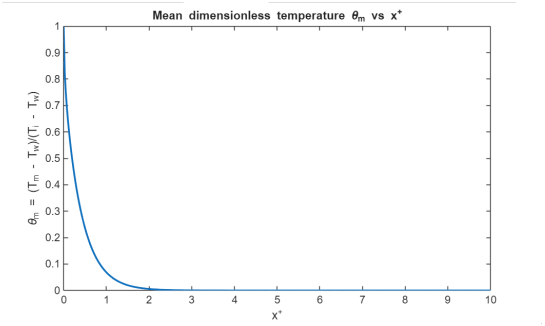


FIGURE 4. Mean dimensionless temperature θ_m vs. x^+

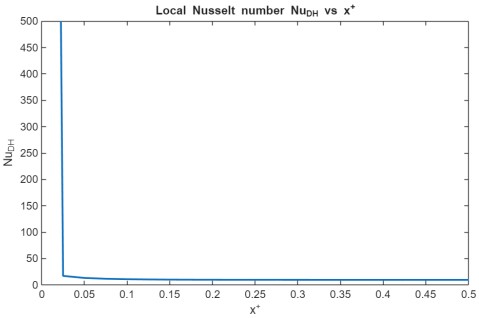


FIGURE 5. Local Nusselt's number Nu_{D_H} vs. x^+

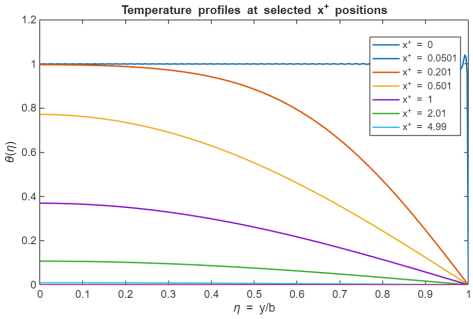


FIGURE 6. Temperature profile plots for various values of x^+

CONCLUSION

This study presented an analytical solution for the transient convective heat transfer in laminar slug flow between parallel plates subjected to a constant wall temperature. By employing an eigenfunction expansion, the dimensionless temperature field was expressed in terms of rapidly converging Fourier–cosine series, enabling evaluation of local and mean temperature distributions as functions of the dimensionless axial coordinate x^+ and the dimensionless transverse coordinate η. The derived expressions for the dimensionless mean temperature $\theta_m(x^+)$ and the local Nusselt number $Nu_{D_H}(x^+)$ clearly demonstrate the thermal development process along the flow direction. The temperature profiles reveal that near the inlet region, heat transfer is dominated by conduction across the channel width, while downstream regions exhibit a gradual transition toward a thermally fully developed state. The local Nusselt number is initially high, reflecting strong thermal gradients, and asymptotically approaches a constant value as x^+ increases, consistent with the establishment of a steady thermal boundary layer. The analytical results agree well with classical slug flow correlations and provide valuable benchmark data for validating numerical simulations of developing laminar convection. The solution framework also highlights the strong dependence of thermal development on the dimensionless parameters Re_{D_H} and Pr, through their role in defining $x^+ = \frac{4x}{bRe_{D_H}Pr}$ Overall, this analytical approach offers a rigorous and compact formulation for predicting temperature distributions and heat transfer coefficients in laminar slug flow between parallel plates. The derived relations and visualizations—such as the contour maps and Nusselt number variations produced via MATLAB, enhances physical understanding of thermal development and provide a solid foundation for extending the model to more complex flow geometries, variable wall conditions, or non-Newtonian fluids.

REFERENCES

1. , Onur N. (2023). Index. In Introduction to Convective Heat Transfer, N. Onur (Ed.). https://doi.org/10.1002/9781119766797.index
2. , Kays, W.M., Crawford, M.E., and Weigand, B. (2005). Convective Heat and Mass Transfer. McGraw-Hill.

[1] School of Mechanical and Manufacturing Engineering (SMME), National University of Sciences and Technology (NUST), Islamabad Capital Territory, 44000, Pakistan

Email address: mghauri.ug22smme@student.nust.edu.pk